Enhancing Heavy-Oil-Recovery Efficiency by Combining Low-Salinity-Water and Polymer Flooding

Yang Zhao and **Shize Yin,** Missouri University of Science and Technology; **Randall S. Seright,** New Mexico Petroleum Recovery Research Center; **Samson Ning,** Reservoir Experts, LLC and Hilcorp Alaska, LLC; **Yin Zhang,** University of Alaska Fairbanks; and **Baojun Bai*,** Missouri University of Science and Technology

Summary

Combining low-salinity-water (LSW) and polymer flooding was proposed to unlock the tremendous heavy-oil resources on the Alaska North Slope (ANS). The synergy of LSW and polymer flooding was demonstrated through coreflooding experiments at various conditions. The results indicate that the high-salinity polymer (HSP) (salinity = 27,500 ppm) requires nearly two-thirds more polymer than the low-salinity polymer (LSP) (salinity = 2,500 ppm) to achieve the target viscosity at the condition of this study. Additional oil was recovered from LSW flooding after extensive high-salinity-water (HSW) flooding [3 to 9% of original oil in place (OOIP)]. LSW flooding performed in secondary mode achieved higher recovery than that in tertiary mode. Also, the occurrence of water breakthrough can be delayed in the LSW flooding compared with the HSW flooding. Strikingly, after extensive LSW flooding and HSP flooding, incremental oil recovery (approximately 8% of OOIP) was still achieved by LSP flooding with the same viscosity as the HSP. The pH increase of the effluent during LSW/LSP flooding was significantly greater than that during HSW/HSP flooding, indicating the presence of the low-salinity effect (LSE). The residual-oil-saturation (S_{or}) reduction induced by the LSE in the area unswept during the LSW flooding (mainly smaller pores) would contribute to the increased oil recovery. LSP flooding performed directly after waterflooding recovered more incremental oil (approximately 10% of OOIP) compared with HSP flooding performed in the same scheme. Apart from the improved sweep efficiency by polymer, the low-salinity-induced S_{or} reduction also would contribute to the increased oil recovery by the LSP. A nearly 2-year pilot test in the Milne Point Field on the ANS has shown impressive success of the proposed hybrid enhanced-oil-recovery (EOR) process: water-cut reduction (70 to less than 15%), increasing oil rate, and no polymer breakthrough so far. This work has demonstrated the remarkable economical and technical benefits of combining LSW and polymer flooding in enhancing heavy-oil recovery.

Introduction

Heavy-oil resources are abundant and account for a large portion of the total oil reserves around the world. Thermal methods, such as steamflooding, are effective techniques to develop the heavy-oil resources. However, in some areas the thermal methods are not feasible. For example, the Milne Point heavy-oil reservoir on the ANS is thin and covered with a thick permafrost layer. Heat loss and environmental concerns make thermal-recovery methods unacceptable. Solvent-based methods (solvent agent: carbon dioxide, methane, and propane, and/or their mixture) show potential in reducing the in-situ oil viscosity and enhancing the oil recovery (Jiang et al. 2019; Sun et al. 2020). However, the high mobility of the displacing agent would make it challenging to achieve the anticipated EOR performance without additional measures. The cost is also a key concern because a massive amount of relatively expensive solvent is required. Waterflooding can maintain the production at the early stage, but it soon shows premature breakthrough and fast rise of water cut (Kargozarfard et al. 2019). Polymer flooding is believed an effective method to unlock the heavy-oil resources in this area. Successful field applications of polymer flooding in heavy-oil reservoirs have been reported around the world, including in Canada (e.g., Pelican Lake, Seal, Cactus Lake), China (e.g., Bohai Bay), the Middle East, Suriname (e.g., Tambaredjo), and Trinidad and Tobago (Saboorian-Jooybari et al. 2016).

The first-ever polymer-flood pilot test on the ANS has been implemented since August 2018 (Dandekar et al. 2019, 2020; Ning et al. 2019; Wang et al. 2020). Because an LSW resource is readily available in the field and no additional facilities are required, it is possible to combine the advantages of LSW and polymer flooding in a technically and economically attractive way at Milne Point. Despite the convenient implementation of the hybrid EOR process, however, it is challenging to fully understand the physics of the complex polymer/brine/oil/rock system. Systematic laboratory research work is required to verify the synergic effect, identify favorable conditions for implementation, and maximize the oil-recovery performance.

LSW has drawn increasing attention during the last 2 decades since the pioneering work of Morrow and his collaborators (Tang and Morrow 1997, 1999). Various papers have demonstrated encouraging EOR potential in laboratory experiments, pilot tests, and field applications (Sheng 2014; Awolayo et al. 2018; Chavan et al. 2019). The salinity of the injection water should be low enough for the presence of the LSE, usually less than 1,500 ppm, but the LSE has been observed at salinity up to 5,000 ppm (Morrow and Buckley 2011). There is no clear boundary to define the "low" and "high" salinity. In general, the salinity of the injected brine was approximately 5 to 10% of the connate brine (Awolayo et al. 2018). Various mechanisms were proposed in the literature. No consensus is now available on the major mechanism(s) that are responsible for the improved oil recovery during LSW flooding. The most often-discussed mechanisms for sandstone porous media include (Sheng 2014) wettability alteration; multicomponent ion exchange; clay swelling, fines destabilization and migration; salt-in effect; osmosis pressure; and alkaline-like flooding.

Several researchers have discussed the technical and economic benefits of combining LSW and polymer flooding. The oil used in the published studies so far has a relatively low viscosity (<50 cp). By using LSW, one of the most direct benefits is significant reduction of the polymer consumption. For example, Vermolen et al. (2014) reported that the required polymer concentration could be reduced by two to four times when using LSW as the makeup brine compared with HSW. Shiran and Skauge (2013) investigated the diluted seawater

*Corresponding author; email: baib@mst.edu

Original SPE manuscript received for review 1 July 2020. Revised manuscript received for review 13 August 2020. Paper (SPE 204220) peer approved 28 August 2020.

as both secondary and tertiary in strongly water-wet and intermediate-wet outcrop Berea Sandstone cores. Also, they tested the low-concentration polymer solution (3630S, 300 ppm, 2.6 cp) in improving oil recovery beyond the residual oil saturation established with diluted seawater. Secondary-mode LSW showed improved oil recovery, especially in intermediate-wet cores, while tertiary-mode LSW only showed a very marginal low-salinity benefit for intermediate-wet cores. The 300-ppm polymer flooding showed no improvement in strong-water-wet cores after secondary or tertiary LSW flooding. An increase in oil recovery of 5% of OOIP was observed in the intermediate-wet cores after tertiary LSW flooding, and 12 to 17% oil-recovery increase after secondary LSW flooding. Kozaki (2012) performed several coreflood experiments to investigate the performance of LSP flooding after waterflooding in aged Berea Sandstone cores. Beneficial recovery was observed from tertiary LSP flooding, both after limited and extensive HSW flooding.

The research reported by Eni also demonstrated the EOR potential of LSP over HSP with aged-reservoir-sandstone cores (Moghadasi et al. 2019). Their experiments showed that LSP could achieve 8% additional oil after extensive HSP with the same viscosity. Moreover, the LSP showed remarkable economic benefit because a much lower polymer concentration was used for LSP (300 vs. 1000 ppm). Almansour et al. (2017) performed six coreflooding experiments with Berea and Bentheimer sandstone cores. They reported that in intermediate-wet-sandstone cores (Berea), a tertiary LSP significantly improved the oil recovery, and the improvement was greater after a secondary HSW flood (16.7% after HSW vs. 11.6% after LSW). However, the recovery by LSW and the ultimate recovery was much higher (55.4 vs. 40.3%; 67.0 vs. 57%). They attributed the beneficial LSE to the release of mixed-wet fines, as supported by fines production in effluent and the fluctuation in pressure drop during LSW flooding. The initial wettability had a significant effect on the secondary-LSW recovery rate and efficiency, and on the incremental recovery of the tertiary LSP and the final recovery. Torrijos et al. (2018) studied the effect of the injection scheme on the oil-recovery performance of LSP. In their experiments, an obvious pH increase was observed during the LSP flooding. The beneficial effect of LSP flooding was also reported by a very recent study (Kakati et al. 2020).

However, the reported observations were made from relatively light oils. For example, in the cases discussed previously, the oil viscosity is in the range of 2.4 to 33 cp. In this study, the problems we aim to solve include the following:

- Is the hybrid EOR method of combining LSW and polymer flood effective for a 200-cp heavy oil? To what extent could the hybrid EOR method improve the oil-recovery performance in the target heavy-oil reservoir at Milne Point Field?
- Can the LSP further reduce the residual oil saturation established after extensive waterflooding and/or extensive HSP flooding of the same viscosity?
- What favorable flooding scheme is beneficial to maximizing the synergy effect?
- What are the possible mechanisms responsible for the EOR?

To achieve these goals, a series of coreflooding experiments were performed using representative brine/oil/core materials under various flooding schemes. The possible mechanisms that are responsible for the synergic benefit of combining the LSW and polymer were explored. The performance of the 2-year field pilot test in the target field was also briefly discussed.

Experimental

Brine. The compositions of formation brine and injection brine are shown in **Table 1.** The synthetic formation brine and synthetic injection brine were prepared in the laboratory according to the corresponding brine compositions in Milne Point Field. The salinity of the synthetic injection brine (2,498 ppm) was approximately 9% of the synthetic formation brine (27,500 ppm), and they are regarded as HSW and LSW, respectively, in this paper (Sheng 2014; Awolayo et al. 2018). The ionic strengths of the HSW and LSW are 0.492 and 0.046, respectively.

Name	Properties (Measured at 71°F)	Composition (ppm)
HSW (SFB)	pH=7.30	Na^{+}: 10086.0
	$\mu = 1.15$ cp	K^{+}: 80.2
	TDS = 27,500 ppm	Ca^{2+}: 218.5
	Ionic strength = 0.492	Mg^{2+}: 281.6
	Hardness: 1,700 ppm	Cl^{-}: 16834.4
LSW (SIB)	pH=7.50	Na^{+}: 859.5
	$\mu = 1.07$ cp	K^{+}: 4.1
	TDS = 2498 ppm	Ca^{2+}: 97.9
	Ionic strength = 0.046	Mg^{2+}: 8.7
	Hardness: 280 ppm	Cl^{-}: 1527.6

Table 1—Compositions of formation brine and injection brine. SFB = synthetic formation brine; SIB = synthetic injection brine; TDS = total dissolved solids.

Polymer. The polymer used was an acrylamide-acrylate copolymer, Flopaam® 3630S (Pfizer Inc., New York, New York, USA). This polymer was selected for the pilot polymer-flood project because of the availability and cost of the polymer products, and initial laboratory/numerical studies (Dandekar et al. 2019). The hydrolysis degree was 25 to 30% with a molecular weight of 18 to 20×10^{6} daltons. HSP and LSP were prepared with the HSW and LSW, respectively. Before adding the polymer powder, the brine was deoxygenated with argon. The desired amount of polymer was slowly added into the brine while being stirred with a magnetic bar at 300 rev/min. The solution was stirred at room temperature for approximately 24 hours until all the polymer powders were well-dissolved. The polymer solution was filtered through 1.2-μm filter paper.

Oil. The crude oil was collected at a wellhead at Milne Point Field (Well B-28). The oil sample was centrifuged to remove water and solids (if any) and filtered through 0.5-μm filter paper. The viscosity of the oil was 202 cp at reservoir temperature (71°F), and the °API value was 19.0 (0.940 g/cm^3). A commercial heavy mineral oil (CAS 8042-47-5) was used in one coreflooding experiment. The mineral oil was composed of paraffin oil and had a viscosity of 173 cp, comparable with the crude oil.

Sandpacks. Because proper core plugs were not available, sandpacks prepared with formation sand were applied to perform the coreflooding tests. The sand was from a crushed core sample from the target reservoir formation (Schrader Bluff NB-sand) from Well Liviano-01A at Milne Point. The formation was poorly consolidated, and the core samples were not intact to use directly for coreflooding tests. The sand kept the native condition to some extent, with crude oil attached on the sand surface, as shown in **Fig. 1a.** The sand was used as received to prepare the sandpacks. The sand contained 1.5% illite, 1.5% chlorite, 1% dolomite, approximately 10% albite, and the remaining was quartz. The native-state sand and the scanning-electron-microscope image are shown in Fig. 1. The median size of the sand was approximately 170 μm. The sandpacks were prepared using a steel tube with an inner dimension of 2.54×20.4 cm. A piece of stainless-steel screen was attached to the outlet end plug to prevent sand from being flushed out of the sandpack tube. A wet-packing method was adopted to prepare the sandpacks. The sand was mixed with formation brine and set for approximately 24 hours to remove air bubbles attached on the sand. The sand was slowly added to the sandpack tube at multiple times. A hammer was used to knock the tube body to make sure the sand was well-packed. The pore volume (PV) and porosity were measured through tracer test. After measuring the permeability with formation brine, crude oil was injected to establish the irreducible water saturation (S_{wi}).

(a) Formation sand in native state
(b) Scanning-electron-microscope image of the sand

Fig. 1—Formation sand: (a) Formation sand in native state; (b) scanning-electron-microscope image of the sand.

Rheology Measurement. The viscosity of injected- and produced-brine/polymer solutions was measured with a commercial viscometer for a wide range of shear rate (0.5 to 200 seconds^{-1}) at reservoir temperature. A commercial UL adapter system was used in the measurement. The viscosity of crude oil was also measured. The SC-34 spindle-container system was adopted because of the relatively high viscosity. The deviation of the measurement was within 0.1% of the viscoelasticity of the LSP and HSP. To evaluate the viscoelasticity of the polymer solutions, a commercial rheometer was used to measure the storage modulus (G') and loss modulus (G'') of the polymer solutions through frequency-sweep tests (0.1 to 100 rad/s) in the linear viscoelastic regime. The polymer showed power-law behavior, as shown in **Fig. 2.** As the salinity was reduced, the required polymer concentration decreased to achieve the target viscosity (45 cp). The viscosities of the two polymer solutions were very close to each other. The concentrations of the two polymers were 2,300 and 1,400 ppm, respectively, which indicates the HSP required 64% more polymer than the LSP to achieve the target viscosity. The polymer molecules are more likely in a coiled state in a high-salinity environment. This is a result of the strong repulsive forces exerted by the surrounding dense ions (Muller et al. 1979). Consequently, the viscosifying ability of the polymer molecules is suppressed. On the contrary, the polymer molecules would be in a stretched status and have a greater viscosifying ability at low-salinity conditions.

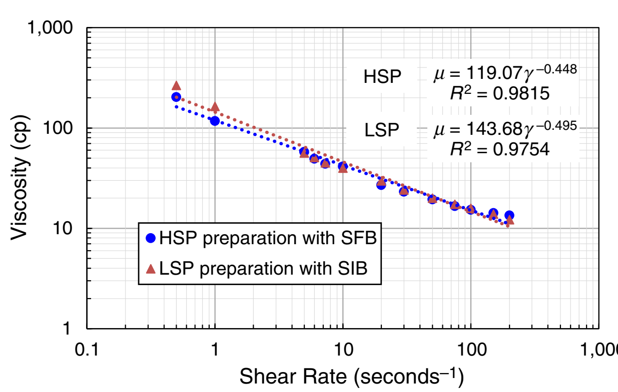

Fig. 2—Polymer viscosity.

pH Measurement. The pH value of the brine, polymer solutions, and aqueous phase of the effluent was measured with a pH meter with an accuracy of ±0.002 pH (Thermo Scientific Orion™ 2-Star Benchtop). The pH values of the injected fresh HSW and LSW were 7.3 and 7.5, respectively. The pH values of the fresh HSP and LSP were 7.6 and 7.8, respectively.

Coreflooding Experiments. Fig. 3 shows the coreflood setup. It consists of a D-series ISCO syringe pump, accumulators, the sandpack assembly, pressure transducers, data-acquisition system, effluent-collection system, and tubing lines and valves. The pump could work in constant-pressure and constant-flow-rate mode. The flow-rate accuracy was 0.001 cm^3/min and the maximum operating pressure was 7,500 psi. A pressure sensor was mounted to monitor the injection pressure at the inlet of the sandpack model. The accuracy of the pressure sensor was within ±0.1%. The effluent samples were collected with graduated tubes at proper frequency. The samples were examined to obtain the oil-recovery information and subject to further test of pH, salinity, and viscosity. Twelve sets of coreflooding experiments were performed **(Table 2).** Experiments 1 and 2 were aimed at investigating LSW flooding performed in tertiary mode and secondary mode, respectively. From these two experiments, we intended to testify whether the low-salinity brine could improve the recovery compared with the high-salinity brine. Also, we would explore the favorable conditions in which the low-salinity benefit could be realized [i.e., is performing the LSW flooding directly (secondary) better or is a tertiary scheme preferable?].

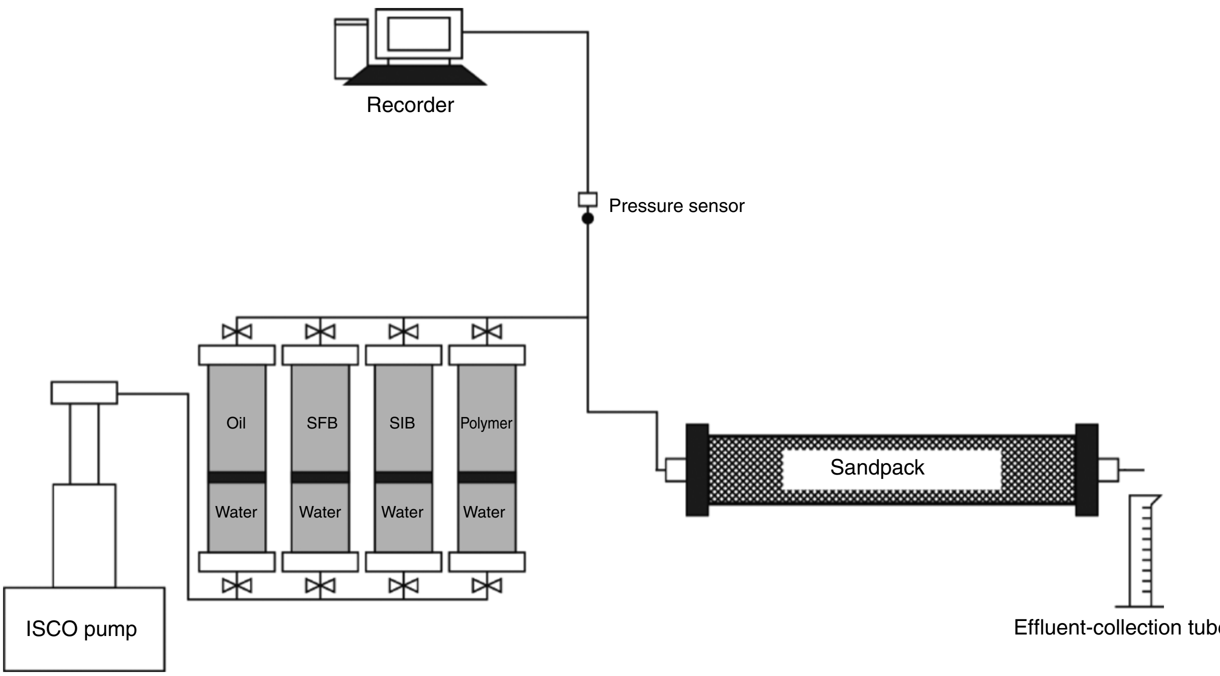

Fig. 3—Coreflooding experiment setup.

Experiment No.	Objective	d (cm)	L (cm)	Porosity	K (md)	S_{wi}	Flooding Process
1	LSW in tertiary mode	2.54	20.40	0.415	1770	0.160	1. HSW flooding to S_{or} 2. LSW flooding to no oil production
1R1	LSW in tertiary mode (reproducibility test)	2.54	20.40	0.453	16,205	0.103	1. HSW flooding to S_{or} 2. LSW flooding to no oil production
1R2	LSW in tertiary mode (reproducibility test)	2.54	20.40	0.316	478	0.109	1. HSW flooding to S_{or} 2. LSW flooding to no oil production
2	LSW in secondary mode	2.54	20.40	0.453	16,205	0.112	1. LSW flooding to no oil production 2. HSW flooding to no oil production
3	HSP flooding after WF	2.54	20.40	0.415	1770	0.160	HSP flooding performed after Experiment 1 until no oil production
3R	HSP flooding after WF (reproducibility test)	2.54	20.40	0.453	16,205	0.112	HSP flooding performed after Experiment 1R1 until no oil production
4	PF as secondary recovery	2.54	20.40	0.236	248	0.261	HSP flooding until no oil production
5	LSP after HSP and WF	2.54	20.40	0.415	1770	0.160	LSP flooding performed after Experiment 3 until no oil production
5R	LSP after HSP and WF (reproducibility test)	2.54	20.40	0.453	16,205	0.112	LSP flooding performed after Experiment 3R until no oil production
6	LSP after secondary HSP flooding	2.54	20.40	0.236	248	0.261	LSP flooding performed after Experiment 4 until no oil production
7	LSP right after waterflooding	2.54	20.40	0.316	478	0.109	LSP flooding performed after Experiment 1R2 until no oil production
8	Effect of oil composition	2.50	30.50	0.372	4906	0.164	1. HSW flooding to S_{or} 2. HSP flooding to no oil production 3. LSP flooding to no oil production

Table 2—Basic information of coreflooding experiments. WF = waterflood; PF = polymer flood.

After having a basic understanding of the behavior associated with the low-salinity fluid, we investigated the more complex polymer flooding under different conditions (Experiments 3 through 8). The questions we intended to answer are the following:

- Can more oil can be recovered with conventional polymer flooding after extensive waterflooding, and to what extent? Can the polymer reduce the residual oil saturation established with extensive waterflooding (Experiments 3 and 3R)?
- As a comparison with Experiment 3, what is the oil-recovery potential if the polymer flooding is performed earlier (without waterflooding before polymer flood) (Experiment 4)?
- Can the LSP further reduce the residual oil saturation established with extensive HSP flooding? What about the EOR potential of the LSP after HSP flooding with the same viscosity (Experiments 5, 5R, and 6)?
- Compared with Experiment 3, could the LSP flood achieve a better EOR performance compared with the HSP flood performed in the same scheme? What are the possible mechanisms that are responsible for the improved recovery (Experiment 7)?

In Experiment 8, a heavy mineral oil, instead of the crude oil, was used. This experiment was intended to study the effect of the oil property (composition) on the oil-recovery performance of LSP. The flow rate in the flooding process was set at 0.1 cm^3/min (equivalent to a Darcy velocity of approximately 1.2 ft/D). Because of the adverse mobility ratio between the displacing phase (water or polymer) and the heavy oil, the displacement is not stable. It is difficult to reach the true residual oil saturation during a heavy-oil-recovery process. In view of this, for each flood process, many PVs of displacing fluid were injected to drive the system to the residual-oil-saturation condition for that fluid. During the last several PVs of injection in each flood process, no oil was produced, which confirmed the completion of the displacement. Increased flow rates were used at the end of a flooding process to check the capillary end effect.

Results and Discussion

The oil-recovery results are summarized in **Table 3.** The results are discussed in the following subsections.

Experiment No.	Secondary Flood	Secondary Oil Recovery(%)	S_{or} After Secondary Flood	Incremental Oil Recovery (%)				Endpoint S_{or}	Endpoint Recovery (%)
				HSW	LSW	HSP	LSP		
1	HSW	37.9	0.522	–	8.7	–	–	0.449	46.6
1R1	HSW	41.4	0.526	–	3.0	–	–	0.499	44.3
1R2	HSW	43.9	0.500	–	5.6	–	–	0.450	49.5
2	LSW	49.4	0.482	0.4	–	–	–	0.479	49.9
3	HSW	37.9	0.522	–	8.7	7.4	–	0.387	53.9
3R	LSW	49.4	0.482	0.4	–	7.7	–	0.417	56.3
4	HSP	71.2	0.213	–	–	–	–	0.213	71.2
5	HSW	37.9	0.522	–	8.7	7.4	8.0	0.320	61.9
5R	LSW	49.4	0.482	0.4	–	7.7	8.1	0.339	64.4
6	HSP	71.2	0.213	–	–	–	5.7	0.171	76.9
7	HSW	43.9	0.500	–	5.6	0.4	10.6	0.351	60.6
8	HSW	48.4	0.431	–	–	13.0	0.7	0.316	62.1

Table 3—Summary of coreflooding experiment results.

LSW Flooding: Tertiary vs. Secondary. Experiments 1 and 2 were conducted to investigate the performance of LSW flooding performed in tertiary mode and secondary mode, respectively. The tertiary LSW flooding was performed at residual oil saturation (S_{or}) condition established after extensive HSW waterflooding. The results are shown in **Figs. 4 through 6.**

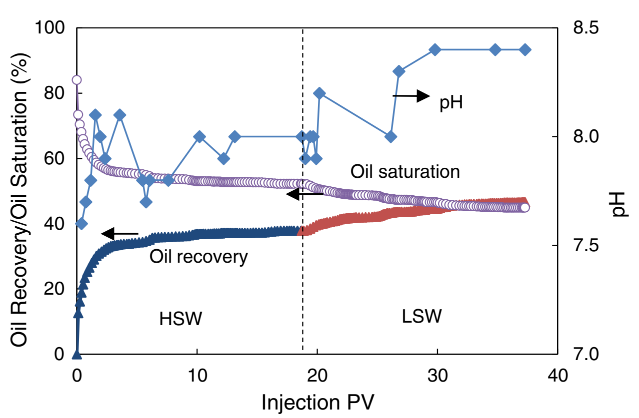

Fig. 4—Tertiary LSW flooding (Experiment 1).

Tertiary LSW Flooding. HSW flooding was first conducted in Experiment 1 as a secondary-recovery method. The water breakthrough occurred at 0.13 PV of injection and 15.2% of the OOIP was recovered. After breakthrough, the water cut quickly increased up to 90% after 0.76 PV of injection. The water cut climbed to 99% after 2.9 PV. However, it took a long time (>15 PV) to visually reach the no-oil-production condition (water cut = 100%). Several additional PVs of water were then injected to confirm that no more oil could be produced. The long tail indicates that the displacement was significantly distorted from a piston-like fashion. It resulted from the adverse mobility ratio between the injected brine and the viscous oil, which can be theoretically supported by the Buckley-Leverett theory (Buckley and Leverett 1942; Pope 1980; Maini 1998). For heavy oil, the displacement process is highly unstable and the water tends to finger into the oil and further develop into channels preferential to water flow between the injectors and producers, as shown in **Figs. 7c and 7d.** A total of 18.7 PV of HSW was injected. The endpoint oil saturation after such extensive flooding (>10 PV) was regarded as the residual oil saturation in this work. This might still not be the exactly true residual oil saturation because of the high viscosity of the oil (Wassmuth et al. 2007). The oil recovery reached 37.9% and the S_{or} was 0.522. Approximately two-thirds of the recovered oil were obtained after water breakthrough.

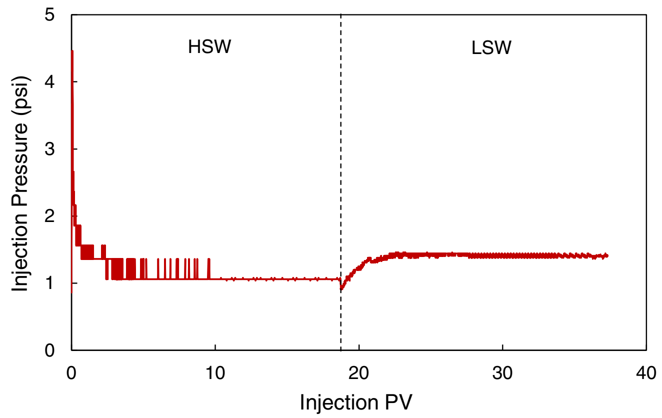

Fig. 5—Injection pressure in Experiment 1.

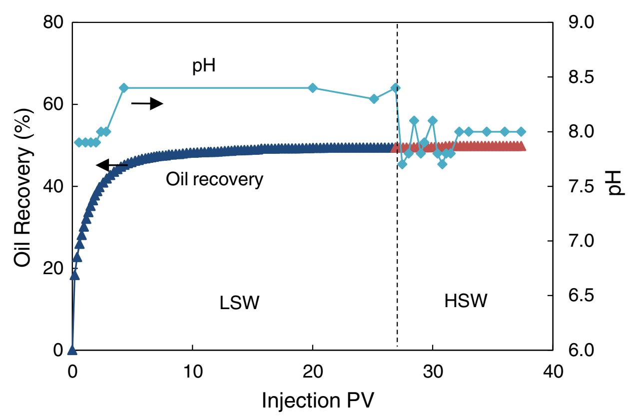

Fig. 6—Secondary LSW flooding (Experiment 2).

After the secondary HSW flooding, extensive PVs of LSW were injected into the core to test whether lowering the salinity could effectively recover more oil after the HSW flooding. The water cut was obviously reduced and 8.7% of OOIP additional oil was recovered. The oil-recovery factor was increased to 46.6%. The results demonstrate the positive effect of low salinity in enhancing the heavy-oil-recovery efficiency. The results are consistent with the recent experimental work, which showed improved oil-recovery performance (6.3% of OOIP) of LSW flooding (total dissolved solids = 3,000 ppm) over HSW flooding (total dissolved solids = 28,000 ppm) for the target Milne Point heavy oil (Cheng et al. 2018).

The capillary end effect was checked according to the Rapoport and Leas (1953) scaling parameter, $Lv\mu$, which should be higher than 3.5 $cm^2 \cdot min^{-1} \cdot cp$ (Qi 2018), where L is the length of the core (in cm); μ is the viscosity of the displacing fluid (in cp); and v is the Darcy velocity (in cm/min). The scaling parameter during waterflooding was 0.43; thus, a capillary end effect was likely. At the end of HSW flooding and LSW flooding, the flow rate was increased to 0.2, 0.5, 1.0, and 2.0 cm^3/min. No additional oil was produced at the increased flow rates. Note that the scaling parameter at 2.0 cm^3/min was 20 times higher and far greater than the critical value. The results indicated that the end effect was negligible.

Experiments 1R1 and 1R2 were performed following the same procedure on different sandpacks (see Appendix A) to test the reproducibility. The results show that LSW recovered more oil after the normal-salinity water. The improvement was quite significant, and an oil incremental of 3.0 and 5.6% of OOIP was achieved, respectively. The oil-recovery efficiency increased from 41.4 to 44.3% for Experiment 1R1, and from 43.9 to 49.5% for Experiment 1R2. Accordingly, the residual oil saturation was significantly reduced. The results further confirmed the positive effect of low salinity on the oil-recovery performance.

Secondary LSW Flooding. In Experiment 2, the sandpack was directly flooded using LSW as the secondary-recovery method. The water breakthrough occurred at 0.18 PV and 20.0% of OOIP was recovered. The breakthrough occurred later, and more oil could be recovered compared with the secondary HSW flooding in Experiment 1. The water cut increased up to 90% after 0.96 PV of injection, and further rose up to 99% after 4.9 PV. The production duration at the relatively lower water-cut level lasted remarkably longer than the secondary HSW flooding. The behavior indicates that the displacement was more stable during the LSW flooding. A total of 27 PV of LSW was injected. Compared with the secondary HSW flooding, the secondary LSW flooding achieved a higher recovery efficiency (49.4 vs. 37.9%) and drove the core to a lower S_{or} (0.482 vs. 0.522). The LSW flooding could recover 8% more oil than the HSW flooding using the same sandpack. Tertiary HSW flooding after the LSW flooding was attempted, but no appreciable incremental oil recovery was observed, as shown in Fig. 6. The overall oil recovery after the tertiary flooding was 49.9%, which was higher than that in Experiment 1R1 (44.3%). Considering the breakthrough behavior and oil-recovery efficiency, the results suggest that the LSW flooding can achieve a better performance than the HSW flooding, and the secondary LSW flooding is better than that performed in the tertiary stage. The results are qualitatively consistent with the observations reported by Shiran and Skauge (2013). They suggested that a secondary LSW was better than a tertiary one because during the secondary HSW flooding, the residual oil was trapped in the pore-throat structures in the swept area. The tertiary LSW tended to follow the water pathways, and thus the oil-recovery performance was not as good as the secondary LSW. Also, the snap-off events were weakened during a secondary LSW flood. For heavy oil, because of the unfavorable mobility ratio, the bypassed oil is expected to be significant after waterflooding. Therefore, the tertiary LSW still has a better chance to recover additional oil compared with the cases with less-viscous oil, as in Shiran and Skauge (2013).

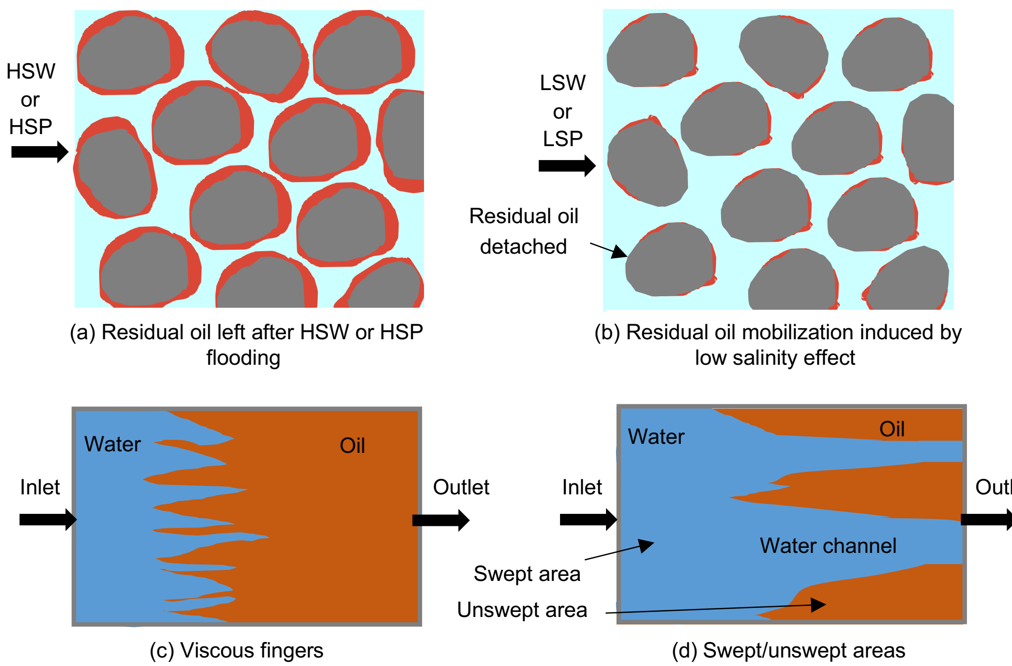

Fig. 7—Residual oil mobilization induced by LSE and the development of preferential water channels. (a) Polar components attach on the sand surface and residual oil is left after HSW or HSP flooding. (b) The residual oil is detached from the sand surface induced by the LSE during LSW or LSP flooding. (c) The water fingers into the oil phase as a result of the adverse mobility ratio between the water and oil phases. (d) Local heterogeneities can exacerbate the viscous fingering, and some parts would be left unswept.

As shown in Fig. 5, the injection pressure during LSW flooding was higher than that during HSW flooding, and no fines production was observed during the entire flooding process. It suggests the low-salinity fluid did not result in formation damage and ruin the injectivity. Also, in the target oil field, LSW flooding had been performed before the polymer-flood pilot test (see the Field-Application Evaluation subsection). For the polymer-flood pilot test, the polymer solution was prepared with LSW that had the same salinity as used in the coreflooding experiments. The low salinity did not induce formation damage during the waterflooding or polymer flooding (Ning et al. 2019). The increased injection pressure might be caused by the wettability alteration induced by the ion exchange and the release of polar components from the pore surfaces. The relative permeability was reduced, as supported by the decreased endpoint relative permeability of water at the S_{or} condition.

The pH change of the produced aqueous phase in Experiments 1 and 2 was plotted in Figs. 4 and 6. As shown in Fig. 4, the pH was stabilized at 8.0 during HSW flooding, while during the tertiary LSW flooding, the pH quickly increased from 7.9 to greater than 8.2 and gradually stabilized at 8.4, which was almost 1.0 pH unit higher than the injected value. The major pH increase synchronized well with the incremental oil-recovery process. A similar trend was observed in Experiment 2, as shown in Fig. 6. The pH increase indicates the presence of an LSE (RezaeiDoust et al. 2011; Shiran and Skauge 2013). The native-state reservoir sand was relatively oil-wet because the sand had contacted the oil for millions of years (Fig. 1). At the initial stage, polar components of the crude oil were adsorbed onto the pore surface either directly or through divalent cations. The cations acted as a bridge to attach the polar components onto the pore surface (mainly the clay surfaces). The adsorbed oil films could not be detached from the sand surfaces by the HSW, which was the same with the connate brine (Fig. 7a). The invasion of LSW disturbed the adsorption-equilibrium status. Ion exchange occurred as a result of the ion-concentration gradient between the invading LSW and the in-situ brine, especially at the pore surfaces. The hydrogen ions were adsorbed onto the surfaces and the divalent cations were released. Also, the hydroxide ions could react with the acidic and basic components through the acid/base reaction (RezaeiDoust et al. 2011); thus, the polar components attached to the pore surface were released. The sand surfaces become more water-wet as the polar components were detached and the oil films became thinner (Fig. 7b). Consequently, the residual oil was mobilized and the residual oil saturation was reduced.

HSP Flooding after Waterflooding. In Experiment 3, the performance of HSP flooding was investigated after extensive HSW flooding and LSW flooding. The results are shown in **Fig. 8.** The results show that the polymer can still improve the oil-recovery performance even after extensive waterflooding (37 PV of HSW and LSW). The oil-recovery incremental was 7.4% of OOIP, and the oil recovery was increased to 53.9%. In the reproducibility-test experiment (Appendix A, Fig. A-3), Experiment 3R, the incremental oil recovery was 6.5% of OOIP, and the oil recovery was increased from 49.9 to 56.3%.

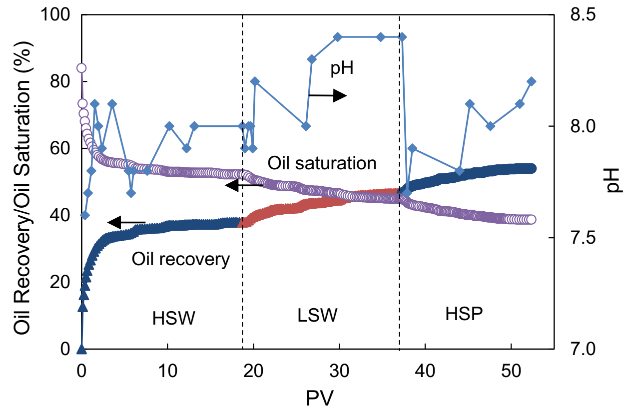

Fig. 8—HSP flooding after waterflooding (Experiment 3).

Because of the adverse mobility ratio during waterflooding, the sweep efficiency is difficult to reach 100%. The adverse mobility ratio would cause fingering problems (Fig. 7c), and local heterogeneity (e.g., pores with different sizes) would make the situation worse because the water prefers to finger into larger pores. The viscous fingers gradually develop into macroscale channels that are preferential to water flow. Afterward, the water mainly transports through the channel from the inlet (injector) to the outlet (producer), as shown in Figs. 7c and 7d. Meanwhile, the oil in smaller pores are bypassed. The core after waterflooding can be divided into two portions (Fig. 7d): the well-swept area (mainly the larger pores) and the unswept area (mainly the smaller pores). The well-swept area is mainly composed of many larger pores and most likely acts as preferential water pathways during waterflooding; thus, this area could be well-swept to the residual-oil-saturation condition. The unswept area primarily consists of smaller pores that are bypassed by the displacing fluid.

After switching to polymer flooding, the mobility-ratio condition is improved and the displacement becomes more stable. Although the polymer is unlikely to mobilize the residual oil in the well-swept area (larger pores) according to the capillary-desaturation curve (Lake et al. 2014; Green and Willhite 2018), the previously bypassed oil left in the unswept area (smaller pores) could be displaced downstream by the viscous-polymer solution. Thus, additional oil could be recovered as the consequence of sweep improvement.

Eq. 1 was used to calculate the capillary number (N_{ca}) of all of flooding processes,

$$N_{ca} = \frac{\mu_w u}{\sigma}, \quad (1)$$

where μ_w is the displacing phase (HSW, LSW, HSP, or LSP) (in mPa·s or cp); u is the superficial velocity (in m/s); and σ is the interfacial tension between the displacing phase and the crude oil (in mN/m). The IFT was measured using a goniometer with the pendant-drop method. The interfacial tension was in the range of 12 to 20 mN/m. The capillary number for the HSW flooding, LSW flooding, HSP flooding, and LSP flooding was 2.46×10^{-7}, 2.39×10^{-7}, 12.5×10^{-6}, and 16.0×10^{-6}, respectively.

Secondary Polymer Flooding. In Experiment 4, the HSP flooding was performed in a secondary mode, as shown in **Fig. 9.** The results indicate much better recovery performance compared with the case preflushed with water (Experiments 3 and 3R). After the secondary polymer flooding, the oil-recovery factor was 71.2%, whereas in Experiments 3 and 3R, the oil recovery after polymer flood was 53.9 and 56.3%, respectively. The experiment indicates that performing the polymer flood earlier can achieve a significantly better oil-recovery performance.

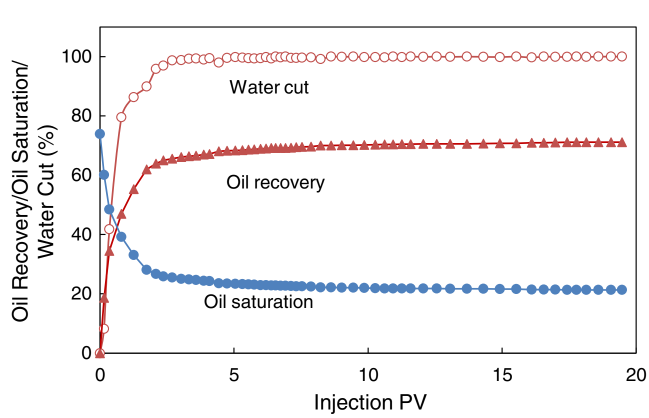

Fig. 9—Secondary polymer flooding (Experiment 4).

The results can be explained with Fig. 7. The viscous fingers could be mitigated and the breakthrough was delayed. The snap-off events of the oil columns while transporting through the pore throats were weakened and delayed during a secondary polymer flooding compared with waterflooding. This interpretation can be supported by the theoretical modeling work of Huh and Pope (2008). In a secondary polymer flood, the oil is in a continuous state and can be displaced downstream more uniformly. The oil columns are more stable and the breakage into small oil drops and/or ganglia can be effectively delayed. The elasticity can make the oil columns become thinner before breakage. Most of the pore space could be well-swept, and the unswept area could be minimized. Higher oil recovery could be achieved at the breakthrough. In Experiment 4, the polymer solution broke through at 0.25 PV, which was significantly later than that in waterflooding. Also, the oil recovery at the breakthrough was approximately 27%, which was nearly double of the HSW flooding in Experiment 1. The water cut increased to 90% at 1.74 PV of injection and the oil recovery was 62%, indicating more stable displacement and better timing benefit of the earlier implementation of polymer flooding.

If the core has been flooded with water (e.g., in Experiment 3), the oil left in the well-swept area would be present as isolated drops or ganglia, which can be trapped by capillary forces and are difficult to mobilize. The mobilization of residual oil in such fashion requires a high capillary number that is greater than a certain critical point, usually on the order of 10^{-5} (Green and Willhite 2018). However, the capillary number for a normal waterflooding is usually on the order of 10^{-7}. According to the capillary-desaturation curve, the capillary number must be increased by several orders of magnitudes after a normal waterflood to mobilize the residual oil and improve the displacement efficiency (Lake et al. 2014; Green and Willhite 2018). A polymer flood is insufficient to provide such a significant increase.

LSP Flooding after Waterflooding and HSP Flooding. In Experiment 5, the performance of LSP flooding was investigated after extensive waterflooding and HSP flooding, as shown in **Fig. 10.** Strikingly, even after extensive flooding with HSP, significant incremental oil was achieved when injecting LSP. Although the viscosity was nearly the same with the HSP and the concentration was significantly lower, the oil-recovery incremental was remarkable (8.0% of OOIP) and the overall oil-recovery factor reached 61.9%. The reproducibility was tested in Experiment 5R, and additional oil of 8.1% of OOIP was achieved and the oil recovery was increased to 64.4%. The pH was increased during the LSP flooding, especially at the early stage, which synchronized well with the incremental oil recovery. The pH increase indicates that ion exchange took place during the flooding process (RezaeiDoust et al. 2011). Inductively coupled plasma analysis could directly give the information of the ion change in the effluent. However, because the samples contained polymer and were highly viscous, the inductively coupled plasma test was not performed. Note that the core had already been exposed to the low-salinity invading fluid during the flooding process with LSW, as shown in Fig. 10. The LSE (e.g., ion exchange, polar-component desorption, and wettability alteration) had already taken effect in the pores that were swept by the LSW (the well-swept area in Fig. 7d). However, there was still an appreciable portion of oil left in the unswept area after the LSW flooding. Although the sweep efficiency was increased and additional oil could be displaced out during the HSP flooding (7.4% of OOIP), still the residual oil saturation could be reduced by the LSE in the area previously untouched by the LSW (Figs. 7b and 7d). As shown in Fig. 10, incremental oil recovery was achieved during the following LSP flooding. The results demonstrate the synergic effect of LSW and polymer flooding in enhancing the heavy-oil recovery.

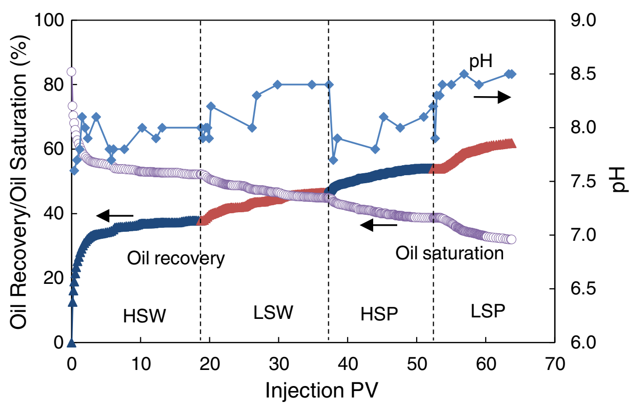

Fig. 10—LSP flooding after waterflooding and HSP flooding (Experiment 5).

To evaluate the mechanical stability as the polymer solutions transport through the sandpacks, we monitored the viscosity of the aqueous effluent during the LSP flooding and HSP flooding. The aqueous phase was obtained by centrifuging the polymer/oil-mixture effluent. **Fig. 11** shows the relative viscosity of the effluent vs. the injected PVs of the HSP and LSP in Experiment 5. The low value at the beginning is caused by the displacement of water present in the porous media. We observed that the LSP could almost reach the injected value, and the mechanical degradation was negligible. For the HSP, the effluent reached 90% of the injected value after several PVs of injection. This indicates that the HSP went through some mechanical degradation, which was probably caused by the coiled configuration of the polymer molecules.

LSP Flooding after a Secondary HSP Flooding. In Experiment 6, the LSP flooding was performed after the secondary polymer flood in Experiment 4. The results are shown in **Fig. 12.** The incremental oil recovery was 5.7% of OOIP. The overall oil recovery was increased to 76.9% after the LSP flooding. The residual oil saturation was reduced from 0.21 to 0.17. The pH of the effluent was increased during the LSP flooding This phenomenon indicated the presence of the LSE, which would contribute to the improved oil recovery. Further discussions of the results are presented in the subsection LSP Flooding Directly after Waterflooding.

LSP Flooding Directly after Waterflooding. In Experiment 7, the LSP flooding was performed after extensive waterflooding (including HSW flooding and LSW flooding). The results are shown in **Fig. 13.** The oil-recovery factor reached 60.1% after the LSP flooding, and an 10.6% of additional oil was recovered in this process. The incremental recovery was higher than the LSP flooding after extensive waterflooding and HSP flooding (Experiments 5 and 5R) and was nearly double that after secondary HSP flooding (Experiment 6). The LSP flooding performed in this scheme was also better than the HSP flooding, as observed in Experiments 3 and 3R, in which the incremental recovery of HSP flooding after extensive waterflooding was 7.4 and 6.5% of OOIP, respectively. Some researchers reported considerable incremental oil recovery and S_{or} reduction in a high-salinity polymer flood after an LSP flood (Qi et al. 2017; Erincik et al. 2018). Their impressive observations might be related to the viscoelasticity effect of the polymer solution present at high-shear-rate condition. It might also be caused by other specialized conditions associated with their experiments (e.g., core conditioning). Our experiments performed at normal flow velocity, as in the reservoir (approximately 1.2 ft/D); however, no appreciable incremental recovery was observed in the HSP flooding after the LSP flooding, indicating that the injection scheme has an important effect on the oil-recovery performance.

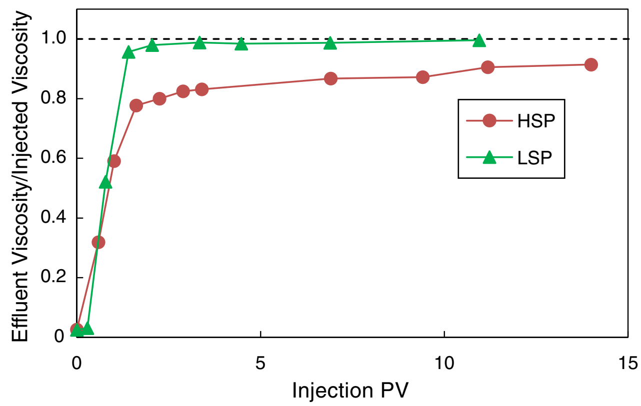

Fig. 11—Relative viscosity of the effluent of HSP and LSP (Experiment 5).

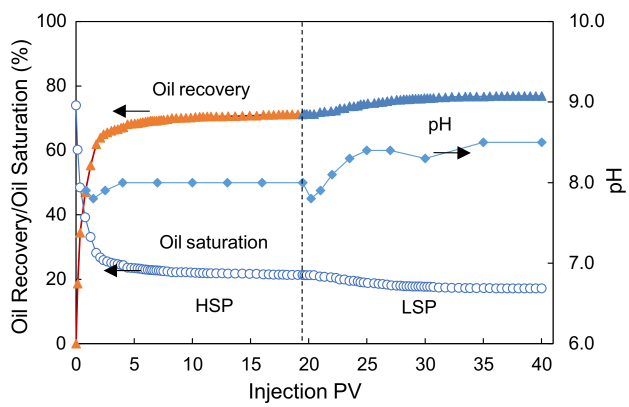

Fig. 12—LSP flooding after a secondary HSP flood (Experiment 6).

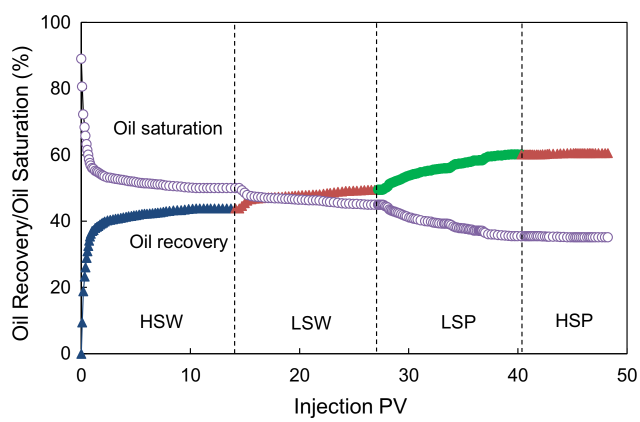

Fig. 13—LSP flooding directly after waterflooding (Experiment 7).

The S_{or} reduction induced by the LSE should be responsible for the improved oil-recovery efficiency during the LSP flooding after secondary HSP flooding (Experiment 6). The sweep efficiency in the secondary HSP flooding was higher than that in the HSW flooding and LSW flooding in Experiment 7. Thus, most of the pore space in the core was well-swept. Further improvement in sweep is expected to be minimal in the following LSP flooding because of the similar viscosity of the two polymer solutions. The incremental recovery was not as significant as the case of LSP flooding after waterflooding (Experiment 7). In the latter case, there was still a considerable portion in the core that was unswept after the waterflooding (mainly the smaller pores). The LSP had a better chance to achieve additional oil recovery through both sweep improvement and S_{or} reduction induced by the low-salinity effect in the unswept area (Fig. 7).

By contrast, the low-salinity-induced reduction mechanism for S_{or} was absent in the HSP flooding (Experiments 3 and 3R); thus, the oil-recovery improvement was not as significant as the LSP flooding in Experiment 7. Note that the sandpack had already been flooded with LSW. Further reduction of the S_{or} was unlikely in the well-swept area (mainly the larger pores). Also, the oil-thread/column-stabilization effect was favorable for the polymer to establish a lower residual oil saturation because the oil saturation in the unswept area was higher than the S_{or} after extensive waterflooding. The mechanism was similar to a secondary polymer flood (Huh and Pope 2008).

Some researchers attribute the reduction in residual oil saturation to the viscoelasticity of the polymer solution (Wang et al. 2000; Koh et al. 2018; Qi 2018; Azad and Trivedi 2020). But viscoelasticity is only significant at a high-shear-rate condition, as indicated by the shear-thickening effect at high flux (Seright 2011; Seright et al. 2011). The linking between the viscoelasticity property and the S_{or} reduction has not been well-understood so far. Also, it is challenging to quantify the representative viscoelasticity property of the polymer solutions in porous media. Some reviews and experimental work have been reported recently (Azad and Trivedi 2019a, 2019b, 2020; Jouenne and Heurteux 2020). We conducted rheology tests to evaluate the viscoelasticity of the LSP and HSP. Frequency-sweep tests (0.1 to 100 rad/s) were performed to measure the storage modulus (G') and loss modulus (G'') with a rheometer in the linear viscoelastic regime. The measured G' and G'' of the LSP and HSP are shown in **Figs. 14 and 15,** respectively. The relaxation times of the polymer solutions were determined with the crossover-point method described in Delshad et al. (2008). The relaxation time for the LSP was 0.633 seconds, which was approximately eight times that of the HSP (0.084 seconds). The result is consistent with the theoretical and experimental results of polymer solutions prepared with 0.1 and 1% sodium chloride reported by Delshad et al. (2008) and Yuan (1981). However, more work is required to clarify the role of the viscoelasticity property in the improved oil recovery and reduced residual oil saturation during the LSP flooding performed at relatively low-velocity conditions.

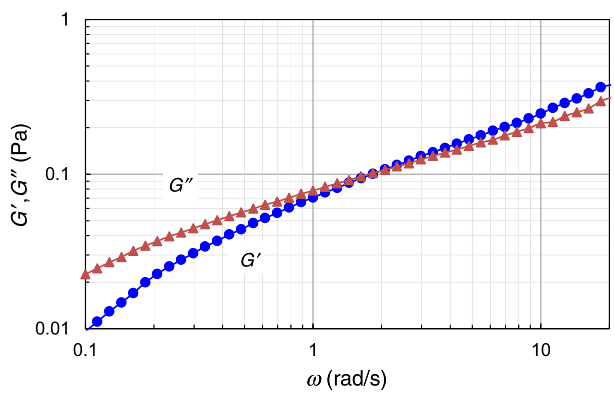

Fig. 14—Rheology-test results of the LSP.

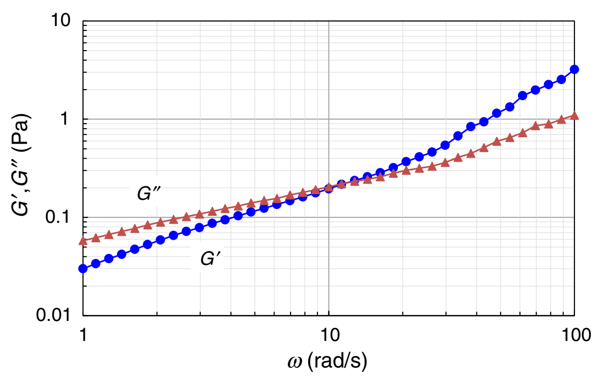

Fig. 15—Rheology-test results of the HSP.

Nevertheless, the results clearly demonstrate that the combination of LSW and polymer flooding can significantly improve the oil-recovery performance. The residual resistance factors (the ratio of water-injection pressure after and before the polymer flooding) of both LSP and HSP were less than 1.5, indicating that injectivity loss and formation damage were not a concern during the polymer flooding.

Field-Application Evaluation. The idea of combining LSW and polymer flooding has been put into practice on a pattern-scale pilot test in Milne Point Field on the ANS. The flood pattern consists of two horizontal injection wells and two horizontal producers. Detailed field practice can be found in Dandekar et al. (2019, 2020) and Ning et al. (2019).

The pilot test has been going on for nearly 2 years and the field performance up to the writing of this paper (May 2020) has preliminarily demonstrated the game-changing potential of LSP flood in unlocking the enormous heavy-oil resources in the ANS. The pilot test has shown impressive successful responses **(Figs. 16 and 17):** The injectivity is sufficient to replace the production voidage; the water cut reduced from 70% at the start of LSP flooding to less than 15%; and there is no polymer breakthrough so far. Figs. 16 and 17 also show that the oil rate has reversed the decline trend (as is expected during waterflood) and started to increase because of the injected polymer. Detailed field performance and benefit analysis will be presented in future publications.

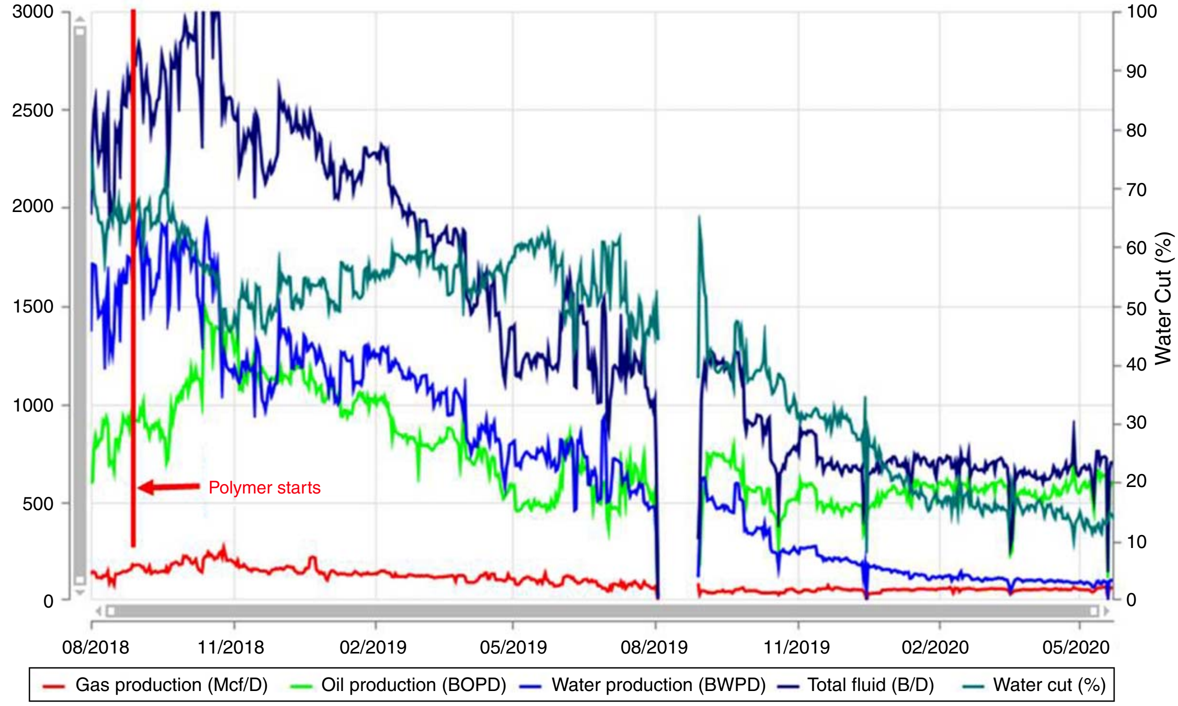

Fig. 16 —Well J-27 production performance. All curves except water cut are to be read on the left vertical axis, using the units in the legend.

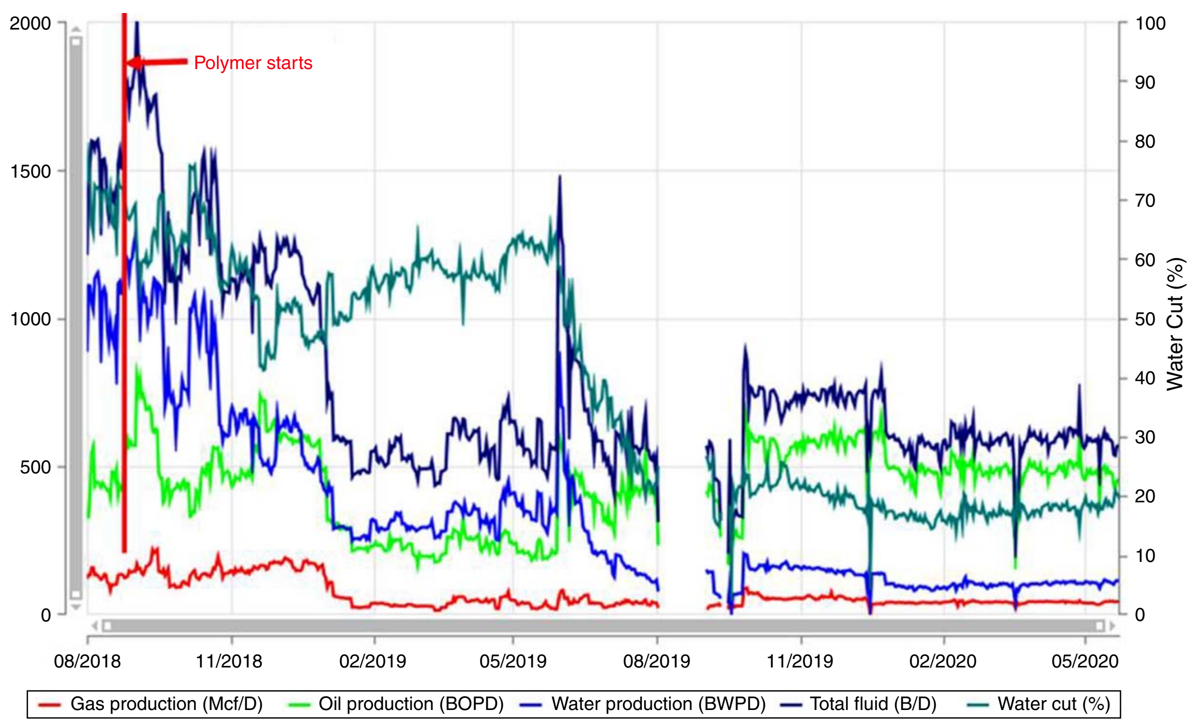

Fig. 17—Well J-28 production performance. All curves except water cut are to be read on the left vertical axis, using the units in the legend.

Discussion of Influencing Factors on the Effectiveness of LSP Flooding. According to our knowledge, the general working conditions required for the LSW should also be satisfied to make the LSP effective. These working conditions have been widely discussed in the literature, including the following:

- The presence of polar components in the crude oil
- The presence of clay in the rock, especially kaolinite
- The presence of connate water (with relatively high salinity)
- The presence of a remarkable amount of divalent ions (Ca^{2+}, Mg^{2+}) in connate water
- The low-salinity injection water
- Relatively low pH values (6 to 7) of the connate brine to allow the adsorption of polar components onto the clay surface (Sheng 2014)

This indicates that the effectiveness of the LSP is governed by multiple factors.

To demonstrate the influence of the oil properties, we performed experiments with heavy mineral oil instead of the crude oil **(Fig. 18).** The viscosity of the mineral oil (173 cp) was comparable with the crude oil (202 cp). Note that LSW flooding was not performed before the LSP flooding. In this circumstance, the LSE during the LSP flooding was expected to be more prominent. However, the results show that no appreciable incremental oil was achieved by the LSP flooding (only 0.73% of OOIP) after extensive HSP flooding. The mineral oil was composed of paraffin oil and contained no polar components. The coreflooding results indicate that the composition of the oil is an important influencing factor on the effectiveness of LSP flooding.

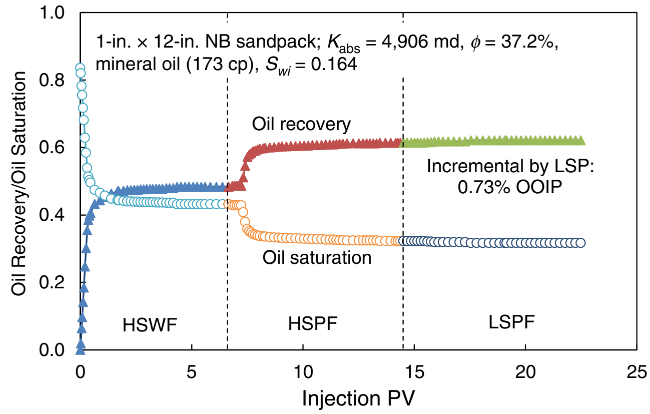

Fig. 18—Coreflooding results using heavy mineral oil.

As for the viscosity of the oil, we consider whether the effectiveness of LSP is selective to heavy or light oil. Several researchers have reported the effectiveness of LSP after limited/extensive waterflooding using crude oil with a lower viscosity (2.4 to 33 cp), as discussed in the Introduction. Kozaki (2012) observed improved oil-recovery performance during LSP flooding after extensive waterflooding. In his experiment, 8% more oil was achieved during LSP flooding after extensive waterflooding using cores of aged Berea Sandstone. Shiran and Skauge (2013) reported 5% oil-recovery increase in LSP flooding after tertiary LSW flooding, and 12 to 17% after secondary LSW flooding in intermediate-wet Berea Sandstone cores. The effectiveness of LSP after extensive HSP with the same viscosity was also reported in the literature ($\mu_o = 25$ to 32 cp; $\mu_p \approx 4$ cp) (Moghadasi et al. 2019). Their experiments showed that LSP could achieve 8% additional oil after extensive HSP with the same viscosity. Our observations with heavy oil showed agreement with the reported results. Our work demonstrates that the efficiency of LSP is not unique to light oil, but it also can be achieved with heavy oil.

It is interesting to know whether the salinity of the LSW/LSP used in the laboratory work of this study and the pilot test is the optimum. Technical and economic considerations should be taken into account in determining the optimal salinity. The salinity of the readily available LSW source in the target field is approximately 2,500 ppm. This is the lowest-possible salinity that available without any further expensive desalination process. Further reducing the salinity requires additional facilities and is technically difficult in the Arctic area. It is possible to obtain medium salinities that are between the formation salinity and source-brine salinity by mixing the produced water with the injection-source brine. However, the problem is that a higher polymer concentration is required to achieve the target viscosity as the salinity is increased. Also, the LSP shows a better mechanical stability, as indicated in Fig. 11. The operation at this lowest-possible salinity shows no injectivity problem in the experiments or the field practice. Therefore, from the technical and economic point of view, the salinity used in this paper is the optimal salinity for the given heavy-oil/brine/rock system.

In this work, we only tested the 3630S polymer, as used in the field pilot test. The choice of this polymer was initially determined by numerical simulation, the availability, and cost of the polymer products (Dandekar et al. 2019). Our project team has investigated the retention behavior of Flopaam 3430S, which has a lower molecular weight of 10 to 12×10^6 daltons (Wang et al. 2020). In the near future, we will systematically study the rheological behavior and oil-recovery performance of different polymers.

Conclusions

We draw the following conclusions from the experimental results:

1. The HSP requires nearly two-thirds more polymer than the LSP to achieve the same target viscosity in this study.
2. Additional oil can be recovered from LSW flooding after extensive HSW flooding (3 to 9% of OOIP). LSW flooding performed in secondary mode can achieve a higher recovery than that in tertiary mode. Also, the occurrence of water breakthrough can be delayed in the LSW flooding compared with the HSW flooding.
3. After extensive LSW flooding and HSP flooding, incremental oil recovery (approximately 8% of OOIP) can still be achieved by LSP flooding with the same viscosity as the HSP. The pH increase of the effluent during LSW/LSP flooding is significantly greater than that during HSW/HSP flooding, indicating the presence of the LSE. The reduction in residual oil saturation (S_{or}) induced by the LSE in the area unswept during the LSW flooding would contribute to the increased oil recovery.
4. LSP flooding performed directly after waterflooding can achieve more incremental oil recovery (approximately 10% of OOIP). The improved sweep efficiency by polymer and the low-salinity-induced S_{or} reduction in the unswept area would contribute to the increased oil recovery.
5. The synergy of combining LSW and polymer flooding has been demonstrated under various conditions in this study. Field-application practice has demonstrated remarkable success regarding water-cut reduction, oil-production improvement, and delayed breakthrough behavior. Future work is required to further investigate the rheology behavior under reservoir conditions, polymer retention, in-situ emulsification, and the impact of wettability at varying salinity conditions.

Nomenclature

N_{ca} = capillary number, dimensionless
S_{or} = residual oil saturation, dimensionless
S_{wi} = initial water saturation, dimensionless
u = superficial velocity, m/s
μ_w = viscosity of the displacing phase (HSW, LSW, HSP, or LSP), mPa·s or cp
σ = interfacial tension between the displacing phase and the crude oil, mN/m

Acknowledgments

"This material is based upon work supported by the Department of Energy under Award Number DE-FE0031606."

Disclaimer: "This report was prepared as an account of work sponsored by an agency of the United States Government. Neither the United States Government nor any agency thereof, nor any of their employees, makes any warranty, express or implied, or assumes any legal liability or responsibility for the accuracy, completeness, or usefulness of any information, apparatus, product, or process disclosed, or represents that its use would not infringe privately owned rights. Reference herein to any specific commercial product, process, or service by trade name, trademark, manufacturer, or otherwise does not necessarily constitute or imply its endorsement, recommendation, or favoring by the United States Government or any agency thereof. The views and opinions of authors expressed herein do not necessarily state or reflect those of the United States Government or any agency thereof."

The authors would like to thank Hilcorp Alaska, LLC, and BP Exploration (Alaska), Inc., for cosponsoring and supporting this project. The valuable help and suggestions from Abhijit Dandekar, Dongmei Wang, and the other members associated with the Department of Energy under Grant No. DE-FE0031606 are sincerely acknowledged. We appreciate Hilcorp for providing the oil, core, and brine materials used in this study.

References

Almansour, A. O., AlQuraishi, A. A., AlHussinan, S. N. et al. 2017. Efficiency of Enhanced Oil Recovery Using Polymer-Augmented Low Salinity Flooding. *J Petrol Explor Prod Technol* **7** (4): 1149–1158. https://doi.org/10.1007/s13202-017-0331-5.

Awolayo, A. N., Sarma, H. K., and Nghiem, L. X. 2018. Brine-Dependent Recovery Processes in Carbonate and Sandstone Petroleum Reservoirs: Review of Laboratory-Field Studies, Interfacial Mechanisms and Modeling Attempts. *Energies* **11** (11): 3020. https://doi.org/10.3390/en11113020.

Azad, M. S. and Trivedi, J. J. 2019a. Novel Viscoelastic Model for Predicting the Synthetic Polymer's Viscoelastic Behavior in Porous Media Using Direct Extensional Rheological Measurements. *Fuel* **235** (1 January): 218–226. https://doi.org/10.1016/j.fuel.2018.06.030.

Azad, M. S. and Trivedi, J. J. 2019b. Quantification of the Viscoelastic Effects during Polymer Flooding: A Critical Review. *SPE J*. **24** (6): 2731–2757. SPE-195687-PA. https://doi.org/10.2118/195687-PA.

Azad, M. S. and Trivedi, J. J. 2020. Does Polymer's Viscoelasticity Influence Heavy-Oil Sweep Efficiency and Injectivity at 1 ft/D? *SPE Res Eval & Eng* **23** (2): 446–462. SPE-193771-PA. https://doi.org/10.2118/193771-PA.

Buckley, S. E. and Leverett, M. C. 1942. Mechanism of Fluid Displacement in Sands. In *Transactions of the Society of Petroleum Engineers*, Vol. 146, Part I, SPE-942107-G, 107–116. Richardson, Texas, USA: Society of Petroleum Engineers.

Chavan, M., Dandekar, A., Patil, S. et al. 2019. Low-Salinity-Based Enhanced Oil Recovery Literature Review and Associated Screening Criteria. *Pet. Sci*. **16** (6): 1344–1360. https://doi.org/10.1007/s12182-019-0325-7.

Cheng, Y., Czyzewski, W., Zhang, Y. et al. 2018. Experimental Investigation of Low Salinity Waterflooding To Improve Heavy Oil Recovery from the Schrader Bluff Reservoir on Alaska North Slope. Paper presented at the OTC Arctic Technology Conference, Houston, Texas, USA, 5–7 November. OTC-29117-MS. https://doi.org/10.4043/29117-MS.

Dandekar, A., Bai, B., Barnes, J. et al. 2019. First Ever Polymer Flood Field Pilot—A Game Changer To Enhance the Recovery of Heavy Oils on Alaska's North Slope. Paper presented at the SPE Western Regional Meeting, San Jose, California, USA, 23–26 April. SPE-195257-MS. https://doi.org/10.2118/195257-MS.

Dandekar, A., Bai, B., Barnes, J. et al. 2020. First Ever Polymer Flood Field Pilot To Enhance the Recovery of Heavy Oils on Alaska's North Slope—Pushing Ahead One Year Later. Paper prepared for publication at the SPE Western Regional Meeting, Bakersfield, California, USA, 20–22 April 2021. SPE-200814-MS. https://doi.org/10.2118/200814-MS.

Delshad, M., Kim, D. H., Magbagbeola, O. A. et al. 2008. Mechanistic Interpretation and Utilization of Viscoelastic Behavior of Polymer Solutions for Improved Polymer-Flood Efficiency. Paper presented at SPE Symposium on Improved Oil Recovery, Tulsa, Oklahoma, USA, 20–23 April. SPE-113620-MS. https://doi.org/10.2118/113620-MS.

Erincik, M. Z., Qi, P., Balhoff, M. T. et al. 2018. New Method To Reduce Residual Oil Saturation by Polymer Flooding. *SPE J*. **23** (5): 1944–1956. SPE-187230-PA. https://doi.org/10.2118/187230-PA.

Green, D. W. and Willhite, G. P. 2018. *Enhanced Oil Recovery*, second edition. Richardson, Texas, USA: Society of Petroleum Engineers.

Huh, C. and Pope, G. A. 2008. Residual Oil Saturation from Polymer Floods: Laboratory Measurements and Theoretical Interpretation. Paper presented at the SPE Symposium on Improved Oil Recovery, Tulsa, Oklahoma, USA, 20–23 April. SPE-113417-MS. https://doi.org/10.2118/113417-MS.

Jiang, J., Rui, Z., Hazlett, R. et al. 2019. An Integrated Technical-Economic Model for Evaluating CO_2 Enhanced Oil Recovery Development. *Appl Energy* **247** (1 August): 190–211. https://doi.org/10.1016/j.apenergy.2019.04.025.

Jouenne, S. and Heurteux, G. 2020. Correlation of Mobility Reduction of HPAM Solutions at High Velocity in Porous Medium with Ex-Situ Measurements of Elasticity. *SPE J*. **25** (1): 465–480. SPE-198899-PA. https://doi.org/10.2118/198899-PA.

Kakati, A., Kumar, G., and Sangwai, J. S. 2020. Low Salinity Polymer Flooding: Effect on Polymer Rheology, Injectivity, Retention, and Oil Recovery Efficiency. *Energy Fuels* **34** (5): 5715–5732. https://doi.org/10.1021/acs.energyfuels.0c00393.

Kargozarfard, Z., Riazi, M., and Ayatollahi, S. 2019. Viscous Fingering and Its Effect on Areal Sweep Efficiency during Waterflooding: An Experimental Study. *Pet. Sci*. **16** (1): 105–116. https://doi.org/10.1007/s12182-018-0258-6.

Koh, H., Lee, V. B., and Pope, G. A. 2018. Experimental Investigation of the Effect of Polymers on Residual Oil Saturation. *SPE J*. **23** (1): 1–17. SPE-179683-PA. https://doi.org/10.2118/179683-PA.

Kozaki, C. 2012. *Efficiency of Low Salinity Polymer Flooding in Sandstone Cores*. Master's thesis, University of Texas at Austin, Austin, Texas, USA (May 2012).

Lake, L. W., Johns, R. T., Rossen, W. R. et al. 2014. *Fundamentals of Enhanced Oil Recovery*. Richardson, Texas, USA: Society of Petroleum Engineers.

Maini, B. 1998. Is It Futile To Measure Relative Permeability for Heavy Oil Reservoirs? *J Can Pet Technol* **37** (4): 56–62. PETSOC-98-04-06. https://doi.org/10.2118/98-04-06.

Moghadasi, L., Pisicchio, P., Bartosek, M. et al. 2019. Laboratory Investigation on Synergy Effect of Low Salinity-Polymer Water Injection on Sandstone Porous Media. Paper presented at the Offshore Mediterranean Conference and Exhibition, Ravenna, Italy, 27–29 March. OMC-2019-0868.

Morrow, N. R. and Buckley, J. 2011. Improved Oil Recovery by Low-Salinity Waterflooding. *J Pet Technol* **63** (5): 106–112. SPE-129421-JPT. https://doi.org/10.2118/129421-JPT.

Muller, G., Laine, J. P., and Fenyo, J. C. 1979. High-Molecular-Weight Hydrolyzed Polyacrylamides. I. Characterization. Effect of Salts on the Conformational Properties. *J Polym Sci A Polym Chem* **17** (3): 659–672. https://doi.org/10.1002/pol.1979.170170305.

Ning, S., Barnes, J., Edwards, R. et al. 2019. First Ever Polymer Flood Field Pilot To Enhance the Recovery of Heavy Oils on Alaska's North Slope–Polymer Injection Performance. Paper presented at the SPE/AAPG/SEG Unconventional Resources Technology Conference, Denver, Colorado, USA, 22–24 July. URTEC-2019-643-MS. https://doi.org/10.15530/urtec-2019-643.

Pope, G. A. 1980. Application of Fractional Flow Theory To Enhanced Oil Recovery. *SPE J*. **20** (3): 191–205. SPE-7660-PA. https://doi.org/10.2118/7660-PA.

Qi, P. 2018. *The Effect of Polymer Viscoelasticity on Residual Oil Saturation*. PhD dissertation, University of Texas at Austin, Austin, Texas, USA (May 2018).

Qi, P., Ehrenfried, D. H., Koh, H. et al. 2017. Reduction of Residual Oil Saturation in Sandstone Cores by Use of Viscoelastic Polymers. *SPE J*. **22** (2): 447–458. SPE-179689-PA. https://doi.org/10.2118/179689-PA.

Rapoport, L. A. and Leas, W. J. 1953. Properties of Linear Waterfloods. *J Pet Technol* **5** (5): 139–148. SPE-213-G. https://doi.org/10.2118/213-G.

RezaeiDoust, A., Puntervold, T., and Austad, T. 2011. Chemical Verification of the EOR Mechanism by Using Low Saline/Smart Water in Sandstone. *Energy Fuels* **25** (5): 2151–2162. https://doi.org/10.1021/ef200215y.

Saboorian-Jooybari, H., Dejam, M., and Chen, Z. 2016. Heavy Oil Polymer Flooding from Laboratory Core Floods To Pilot Tests and Field Applications: Half-Century Studies. *J Pet Sci Eng* **142** (June): 85–100. https://doi.org/10.1016/j.petrol.2016.01.023.

Seright, R. S., Fan, T., Wavrik, K. et al. 2011. New Insights into Polymer Rheology in Porous Media. *SPE J*. **16** (1): 35–42. SPE-129200-PA. https://doi.org/10.2118/129200-PA.

Seright, R. S. 2011. Use of Polymers To Recover Viscous Oil from Unconventional Reservoirs. Final scientific/technical report, DOE Award No. DE-NT0006555, US Department of Energy (October 2011).

Sheng, J. J. 2014. Critical Review of Low-Salinity Waterflooding. *J Pet Sci Eng* **120** (August): 216–224. https://doi.org/10.1016/j.petrol.2014.05.026.

Shiran, B. S. and Skauge, A. 2013. Enhanced Oil Recovery (EOR) by Combined Low Salinity Water/Polymer Flooding. *Energy Fuels* **27** (3): 1223–1235. https://doi.org/10.1021/ef301538e.

Sun, X. F., Song, Z. Y., Cai, L. F. et al. 2020. Phase Behavior of Heavy Oil–Solvent Mixture Systems under Reservoir Conditions. *Pet. Sci*. (in press; published online 14 May 2020). https://doi.org/10.1007/s12182-020-00461-x.

Tang, G.-Q. and Morrow, N. R. 1997. Salinity, Temperature, Oil Composition, and Oil Recovery by Waterflooding. *SPE Res Eng* **12** (4): 269–276. SPE-36680-PA. https://doi.org/10.2118/36680-PA.

Tang, G.-Q. and Morrow, N. R. 1999. Influence of Brine Composition and Fines Migration on Crude Oil/Brine/Rock Interactions and Oil Recovery. *J Pet Sci Eng* **24** (2–4): 99–111. https://doi.org/10.1016/S0920-4105(99)00034-0.

Torrijos, I. D. P., Puntervold, T., Strand, S. et al. 2018. An Experimental Study of the Low Salinity Smart Water-Polymer Hybrid EOR Effect in Sandstone Material. *J Pet Sci Eng* **164** (May): 219–229. https://doi.org/10.1016/j.petrol.2018.01.031.

Vermolen, E. C. M., Pingo-Almada, M., Wassing, B. M. et al. 2014. Low-Salinity Polymer Flooding: Improving Polymer Flooding Technical Feasibility and Economics by Using Low-Salinity Make-Up Brine. Paper presented at the International Petroleum Technology Conference, Doha, Qatar, 19–22 January. IPTC-17342-MS. https://doi.org/10.2523/IPTC-17342-MS.

Wang, D., Cheng, J., Yang, Q. et al. 2000. Viscous-Elastic Polymer Can Increase Microscale Displacement Efficiency in Cores. Paper presented at the SPE Annual Technical Conference and Exhibition, Dallas, Texas, USA, 1–4 October. SPE-63227-MS. https://doi.org/10.2118/63227-MS.

Wang, D., Li, C., and Seright, R. S. 2020. Laboratory Evaluation of Polymer Retention in a Heavy Oil Sand for a Polymer Flooding Application on Alaska's North Slope. *SPE J*. **25** (4): 1842–1856. SPE-200428-PA. https://doi.org/10.2118/200428-PA.

Wassmuth, F. R., Green, K., Hodgins, L. et al. 2007. Polymer Flood Technology for Heavy Oil Recovery. Paper presented at the Canadian International Petroleum Conference, Calgary, Alberta, Canada, 12–14 June. PETSOC-2007-182. https://doi.org/10.2118/2007-182.

Yuan, M. 1981. *A Rheological Study of Polymer and Microemulsion in Porous Media*. Master's thesis, University of Texas at Austin, Austin, Texas, USA (May 1981).

Appendix A—Experimental Results of Reproducibility Tests

The results of Experiments 1R1, 1R2, 3R, and 5R, as well as the injection pressure, are shown in **Figs. A-1 through A-5.**

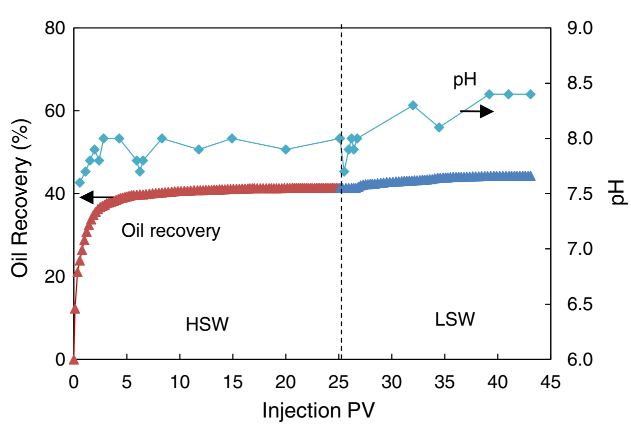

Fig. A-1—Tertiary LSW flooding (Experiment 1R1).

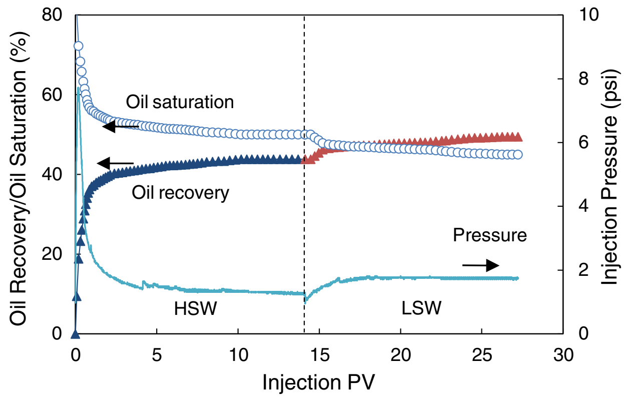

Fig. A-2—Tertiary LSW flooding (Experiment 1R2).

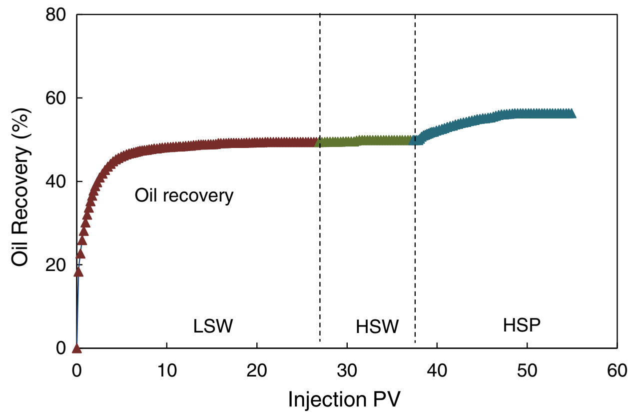

Fig. A-3—HSP flooding after waterflooding (Experiment 3R).

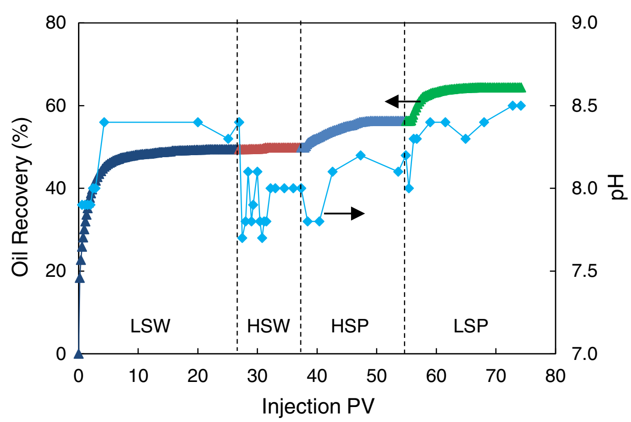

Fig. A-4—LSP flooding after waterflooding and HSP flooding (Experiment 5R).

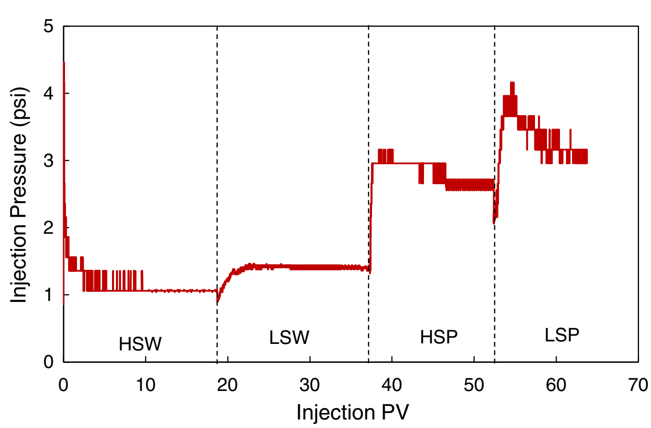

Fig. A-5—Injection pressure in Experiments 1, 3, and 5.

SI Metric Conversion Factors

ft × 3.048*	E−01 = m
md × 9.869233	E−04 = μm^2
psi × 6.8948	E−03 = MPa

*Conversion factor is exact.